



## Study of inclusion complex of $\beta$ -cyclodextrin and diphenylamine: Photophysical and electrochemical behaviors

K. Srinivasan<sup>a</sup>, K. Kayalvizhi<sup>a</sup>, K. Sivakumar<sup>b</sup>, T. Stalin<sup>a,\*</sup>

<sup>a</sup> Department of Industrial Chemistry, Alagappa University, Karaikudi 630 003, Tamilnadu, India

<sup>b</sup> Department of Chemistry, SCSVMV (Deemed University), Kanchipuram 631 561, Tamilnadu, India

### ARTICLE INFO

#### Article history:

Received 25 September 2010

Received in revised form 6 February 2011

Accepted 16 February 2011

#### Keywords:

$\beta$ -Cyclodextrin

Diphenylamine

Inclusion complex

pH effects

Cyclic voltammetry

RasMol tool

### ABSTRACT

The photophysical, electrochemical and photoprototropic behaviors of diphenylamine (DPA) in aqueous  $\beta$ -cyclodextrin ( $\beta$ -CD) solution have been investigated using absorption spectroscopy and cyclic voltammetric techniques. Absorption of the neutral and cationic form of DPA is enhanced due to the formation of a 1:1 complex with  $\beta$ -CD. The formation of this complex has been confirmed by Benesi–Hildebrand plot and docking studies by RasMol tool methods. The solid complex of  $\beta$ -CD with DPA is investigated by FT-IR, XRD and AFM methods. The thermodynamic parameters ( $\Delta G$ ,  $\Delta H$  and  $\Delta S$ ) of inclusion process are also determined. The  $pK_a$  values of neutral-monocation equilibria have been determined with absorption (conjugate acid–base) titrations. A mechanism is proposed to explain the inclusion process.

© 2011 Elsevier B.V. All rights reserved.

### 1. Introduction

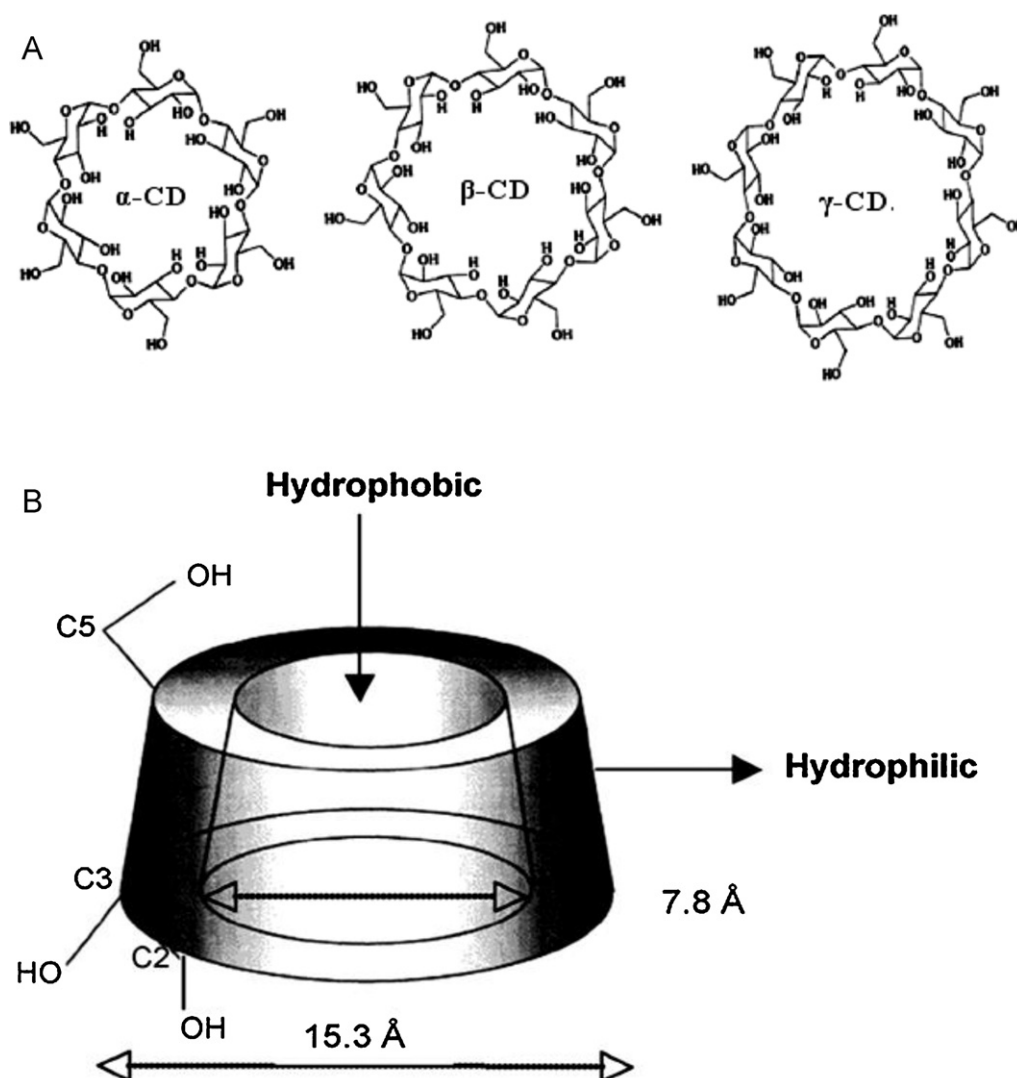
Cyclodextrins (CDs) are cyclic oligosaccharides with internal cavities capable of forming complexes with hydrophobic organic molecules in aqueous solutions [1]. The inner diameters of the cavities are approximately 4.5 Å in  $\alpha$ -CD, 7.0 Å in  $\beta$ -CD and 8.5 Å in  $\gamma$ -CD [2]. The CDs are capable of incorporating a high range of guest molecules based on hydrophobic and geometrical cavities (Scheme 1). They have a toroidal shape with an internal hydrophobic surface and an external hydrophilic surface (Scheme 1) and they are acting as a host molecule. These cyclodextrins are well known as they form stable host–guest inclusion complexes which have the interesting property of including organic, inorganic and biological molecules in their cavities [3,4]. Efforts have been made to modify CDs so as to enhance their catalytic powers [5,6]. The physical chemistry of complexation by CDs has been extensively studied [1–6].

The chemical properties of cyclodextrins combined with their non-toxic character to humans have led to their use in pharmaceuticals, as food additives as well as in the environmental de-contamination procedures of wastewater, aquifer, air, and soil [7,8]. Particularly cyclodextrins and their derivatives have been used to remove contaminations by the formation of inclusion complexes or to enhance the solubility of several compounds [9–12].

Ramamurthy, Eaton, and Co-workers [13,14] have exploited the use of CDs as host to examine photochemical and photophysical processes that occur in molecules complexed within them and to compare their behavior in aqueous solutions and in the solid state. Their studies dealt mostly with intramolecular events, with only a single molecule present in the CD cavity. Furthermore, these studies seem to indicate differences in the extent of inter- and intramolecular hydrogen bond/intramolecular charge transfer for the molecules in aqueous solutions of cyclodextrins. Applications of cyclodextrins and their derivatives cover various areas of the chemistry, including the sensing of organic molecules and organic pollutants, analytical chemistry, pharmaceuticals, food and other industrial areas [15–17].

The inclusion of a guest in a  $\beta$ -CD cavity consists basically of a substitution of the included water molecules by the less polar guest [18]. The process is energetically favoured by the interactions of the guest molecule with the solvated hydrophobic cavity of the host. In this process entropy and enthalpy changes have an important role. In spite of the fact that the “driving force” of complexation is not yet completely understood, it seems that it is the result of various effects [18]; (a) substitution of the energetically unfavoured polar–apolar interactions (between the included water and the  $\beta$ -CD cavity on the one hand, and between water and the guest on the other) by the more favoured apolar–apolar interaction (between the guest and the cavity), and the polar–polar interaction (between bulk water and the released cavity–water molecules). (b)  $\beta$ -CD-ring strain release on complexation, (c) Van der Waals interactions and hydrogen bonds between host and guest molecules.

\* Corresponding author. Tel.: +91 9944266475; fax: +91 4565 225202.  
E-mail address: [tstalinphd@rediffmail.com](mailto:tstalinphd@rediffmail.com) (T. Stalin).



**Scheme 1.** (A) Chemical structures of  $\alpha$ -CD,  $\beta$ -CD and  $\gamma$ -CD. (B) The internal and external widths for  $\beta$ -cyclodextrin are noted in the figure and height of the cavity is presumed to be  $\sim 8 \text{ \AA}$  and width size is  $15.3 \text{ \AA}$ .

In this study, we report the absorption characteristics of diphenylamine (DPA) in different  $\beta$ -cyclodextrin concentrations. For the past one decade, the corresponding author has largely been involved in studying the photophysical properties [19–25] and electrochemical properties [26] of various organic fluorophores. This molecule shows 1:1 inclusion with  $\beta$ -CD molecule, and is clearly confirmed by spectral analysis as well as docking method by RasMol tool [27]. This stimulated us to carry out a study on diphenylamine.

Diphenylamine (DPA) and its derivatives are most commonly used as stabilizers in nitrocellulose-containing explosives and propellants, in the perfumery, and as antioxidants in the rubber and elastomer industry. DPA is also widely used to prevent post-harvest deterioration of apple and pear crops. It is used for the production of dyes, pharmaceuticals, photography chemicals and further small-scale application [28]. First reports showed that DPA was found in soil and groundwater. Some ecotoxicological studies demonstrated the potential hazard of various diphenylamines to the aquatic environment and to bacteria and animals. Studies on the biodegradability of DPA and its derivatives are very sparse. Therefore, further investigation is required to determine the complete dimension of the potential environmental hazard [29] and to introduce possible (bio) remediation techniques for sites that are contaminated with this class of compounds.

Chattopadhyay et al. [30] have studied photochemical conversion of diphenylamine (DPA) to carbazole (CAZL) fluorometrically in aerated aqueous and aqueous  $\beta$ -CD environments. KothaiNayaki et al. [31] have studied the solvatochromism and prototropism of DPA in aqueous solution. The techniques of UV-Vis, FT-IR, XRD, AFM, CV and thermodynamic parameters have been used to examine the effects of  $\beta$ -cyclodextrin upon complexation of diphenylamine. And the formation constants of the complexes were calculated.

## 2. Experimental

### 2.1. Instruments

The absorption spectral (UV-vis spectrum) measurements were carried out with Shimadzu UV-2401PC double-beam spectrophotometer. The pH values in the range 2.0–12.0 were measured using Elico pH meter LI-120. Electrochemical studies were carried out using Auto lab electrochemical analyzer, it used to apply potential on the working electrode equipped with a three-electrode glassy carbon electrode (diameter: 1 mm) is served as a working electrode system. Reference electrode was saturated calomel electrode (SCE) and counter electrode was platinum wire. All experiments were carried out at  $30 \pm 1 \text{ }^\circ\text{C}$ . The working electrode was polished

to a mirror with 0.05  $\mu\text{m}$  alumina aqueous slurry, and rinsed with triply distilled water before each experiment. The supporting electrolyte was pH  $\sim 1$  (0.1 M  $\text{H}_2\text{SO}_4 + 0.1 \text{ M Na}_2\text{SO}_4$ ) and pH  $\sim 7$  (0.1 M  $\text{KH}_2\text{PO}_4 + 0.1 \text{ M NaOH}$ ) buffer. Powder X-ray diffraction spectra were taken by XPert PRO PANalytical diffractometer. FT-IR was recorded using Nicolet 380, Thermo Electron Corporation Spectrophotometer and surface morphology was recorded using AFM diCP-II, veeco USA.

## 2.2. Reagents

$\beta$ -Cyclodextrin ( $\beta$ -CD), were obtained from Sd fine chemical Company} was used without further purification. Diphenylamine (DPA, Loba Chemical Reagents Company) and other chemical reagents were analytical reagent grade. Triply distilled water was used to prepare all solutions. All solvents used were of the highest grade (Spectrograde). Solutions in the pH range 2.0–12.0 were prepared by adding the appropriate amount of NaOH and  $\text{H}_3\text{PO}_4$ . A modified Hammett's acidity scale ( $H_0$ ) [32] for the solutions below pH  $\sim 2$  (using a  $\text{H}_2\text{SO}_4$ – $\text{H}_2\text{O}$  mixture) and Yagil basicity scale ( $H_-$ ) [33] for solutions above pH  $\sim 12$  (using a NaOH– $\text{H}_2\text{O}$  mixture) were employed. The solutions were prepared just before taking measurements. The concentrations of the solutions were of the order ( $10^{-4}$  to  $10^{-5} \text{ mol dm}^{-3}$ ). The stock solution of DPA is  $1 \times 10^{-2} \text{ mol dm}^{-3}$ .

## 2.3. $\beta$ -Cyclodextrin solution preparation

$1 \times 10^{-2} \text{ mol dm}^{-3}$  concentration of stock solution of DPA was prepared using ethanol and 0.2 ml of this stock solution was added into 10 ml volumetric flasks and made up to the mark using the following concentration of  $\beta$ -CD solutions 0, 2, 4, 6, 8, 10 and  $12 \times 10^{-3} \text{ mol dm}^{-3}$  respectively and shaken thoroughly, so that the final concentration of DPA in each flask is  $2 \times 10^{-4} \text{ mol dm}^{-3}$ . All the absorption spectra were recorded at  $30 \pm 1^\circ\text{C}$ .

## 2.4. Preparation of $\beta$ -cyclodextrin solution for electrochemical studies

The stock solution of  $\beta$ -CD ( $12 \times 10^{-3} \text{ mol dm}^{-3}$ ) was prepared using pH  $\sim 1$  (0.1 M  $\text{H}_2\text{SO}_4 + 0.1 \text{ M Na}_2\text{SO}_4$ ) and pH  $\sim 7$  (0.1 M  $\text{KH}_2\text{PO}_4 + 0.1 \text{ M NaOH}$ ) buffer solutions. From the stock solution 2, 4, 6, 8, 10 and  $12 \times 10^{-3} \text{ mol dm}^{-3}$  of  $\beta$ -CD were prepared using pH  $\sim 1$  and pH  $\sim 7$  buffers, so that the final concentration of DPA in each flask is  $2 \times 10^{-4} \text{ mol dm}^{-3}$ . The cyclic voltammograms were recorded after the solution was kept static for at least 24 h.

## 2.5. Preparation of solid inclusion complex of DPA with $\beta$ -CD

Accurately weighed 1 g of  $\beta$ -CD was placed into a 50 ml conical flask and 30 ml triply distilled water was added and then this solution was oscillated enough. After that, 0.15 g DPA was put in to a 50 ml beaker and 20 ml was ethanol added and put over electromagnetic stirrer to be stirred until it was dissolved [34]. Then DPA solutions were slowly poured into  $\beta$ -CD solution. The above-mixed solution was continuously stirred for 48 h at room temperature. The reaction mixture was kept in refrigerator for 48 h. At this time, we observed that white precipitate is formed. The precipitate was filtered by G4 crucible and washed with triply distilled water. After being dried in oven at  $50^\circ\text{C}$  for 12 h, off white powder was obtained. This is solid inclusion complex of DPA with  $\beta$ -CD and it was further analysed by FT-IR, AFM and XRD methods.

**Table 1**

Absorption maxima (nm) and  $\log \epsilon$  of DPA at different concentrations of  $\beta$ -CD in pH  $\sim 1$  and pH  $\sim 7$  solutions.

S.No.	Concentration of $\beta$ -CD (M)	pH $\sim 1$		pH $\sim 7$	
		$\lambda^{\text{max}}$ (nm)	$\log \epsilon$	$\lambda^{\text{max}}$ (nm)	$\log \epsilon$
1	Without $\beta$ -CD	280.0	3.89	279.0	4.03
2	0.002	282.0	4.17	281.5	4.20
3	0.012	283.0	4.18	283.0	4.22
Binding constant ( $\text{M}^{-1}$ )		682		343	
$\Delta G$ ( $\text{kJ mol}^{-1}$ )		–16.4		–14.7	
$\Delta H$ ( $\text{kJ mol}^{-1}$ )		–6436		–6436	
$\Delta S$ ( $\text{kJ mol}^{-1} \text{K}^{-1}$ )		–21.2		–21.2	

## 3. Results and discussion

### 3.1. Effect of $\beta$ -cyclodextrin

The UV–visible absorption spectral data of diphenylamine (DPA) in different concentrations of  $\beta$ -CD are compiled in Table 1. The absorption peaks of DPA ( $1 \times 10^{-4} \text{ mol dm}^{-3}$ ) in pH  $\sim 1$  (Fig. 1) and pH  $\sim 7$  (Fig. 2) appear at 280–283 nm (pH  $\sim 1$ ) and 279–283 nm (pH  $\sim 7$ ). Upon increasing the concentration of  $\beta$ -CD in both cases, no clear isosbestic point is observed in the absorption spectra. In the presence of  $\beta$ -CD, a slight red shift is observed in the absorption maxima at pH  $\sim 1$  (280–283 nm) and a small red shift (279–283 nm) at pH  $\sim 7$ . The absorption spectra show a slight change in absorption maxima even in the presence of the highest concentration of  $\beta$ -CD used ( $12 \times 10^{-3} \text{ mol dm}^{-3}$ ) and there is no change in the absorbance by further addition of  $\beta$ -CD. At pH  $\sim 7$ , DPA exists as a neutral form; hence we also recorded at pH  $\sim 1$  because monocation might be present in acidic condition. The absorption maxima and the spectral shape of DPA molecule in both pHs are almost same, so far there has been no formation of monocation in pH  $\sim 1$ . This behavior has been attributed to the enhanced dissolution of the DPA molecule through the hydrophobic interaction between DPA and  $\beta$ -CD. These results indicated that DPA molecule is entrapped in the  $\beta$ -CD cavity to form 1:1 inclusion complex. In both cases, the binding constant for the formation of DPA– $\beta$ -CD complex has been determined by analyzing the changes in the intensity of absorption maxima with the  $\beta$ -CD concentration. In the case of inclusion complex formed

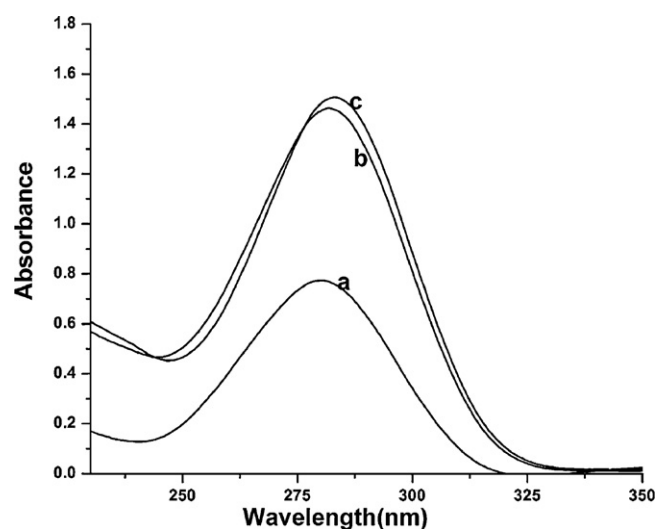


**Fig. 1.** The absorption spectra of DPA (pH  $\sim 1$ ) in different  $\beta$ -CD concentrations (a) 0.0 M, (b) 0.002 M, and (c) 0.012 M.

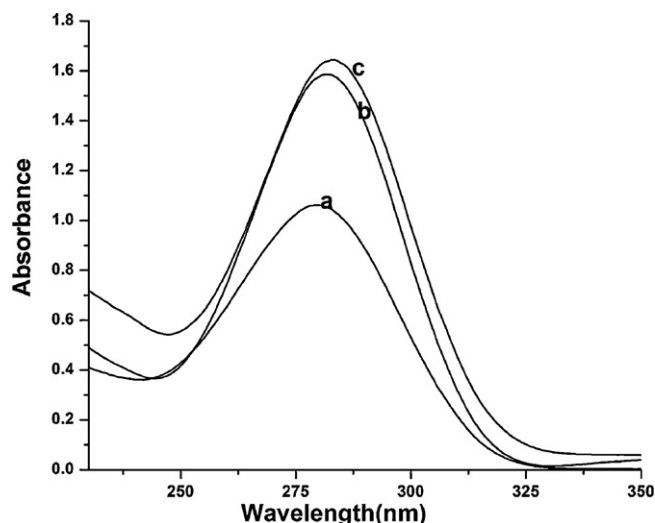


Fig. 2. The absorption spectra of DPA (pH ~7) in different  $\beta$ -CD concentrations (a) 0.0 M, (b) 0.002 M, and (c) 0.012 M.

between DPA and  $\beta$ -CD, the equilibrium can be written as



The binding constant 'K' and stoichiometric ratios of the inclusion complex of DPA can be determined according to the Benesi–Hildebrand [35] relation assuming the formation of a 1:1 host–guest complex.

$$\frac{1}{A - A_0} = \frac{1}{\Delta\varepsilon} + \frac{1}{K[\text{DPA}]_0 \Delta\varepsilon [\beta\text{-CD}]_0}$$

where  $A$  and  $A_0$  are the difference between the absorbance of DPA in the presence and absence of  $\beta$ -CD,  $\Delta\varepsilon$  is the difference between the molar absorption coefficient of DPA and the inclusion complex,  $[\text{DPA}]_0$  and  $[\beta\text{-CD}]_0$  are the initial concentration of DPA and  $\beta$ -CD, respectively. Fig. 3 depicts a plot of  $1/A - A_0$  vs.  $1/[\beta\text{-CD}]$  for DPA (in both pHs) and a good linear correlation was obtained, confirming the formation of a 1:1 inclusion complex. From the intercept and slope values of this plot,  $K$  is evaluated and the binding constants for neutral DPA (pH ~7,  $343 \text{ M}^{-1}$ ) are considerably less than those of its acidic condition form (pH ~1,  $682 \text{ M}^{-1}$ ) at 303 K. The binding constants are sensitive to change in the pH values, which reveal that selective inclusion associated with the species form (neutral and acidic condition) of DPA.

The determination of the thermodynamic parameters in this inclusion process in the free energy change can be calculated from the binding constant 'K' by the following equation

$$\Delta G = -RT \ln K$$

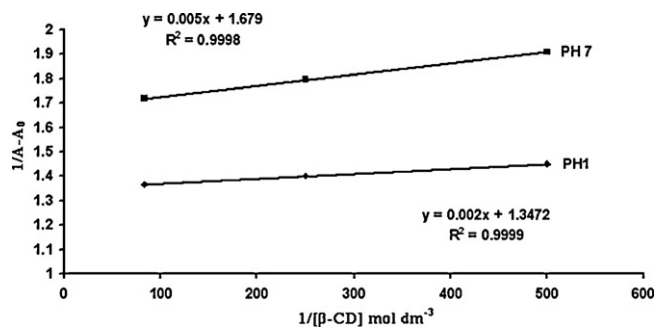
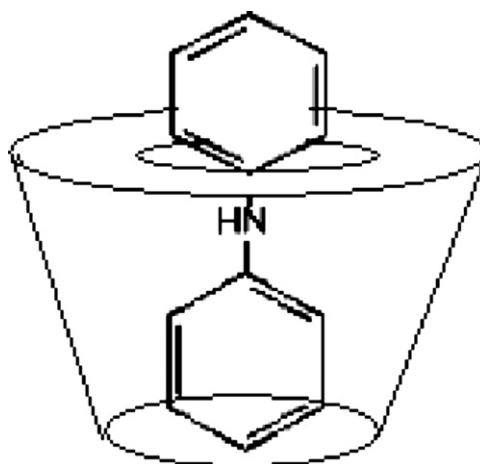


Fig. 3. Benesi–Hildebrand plot of  $1/A - A_0$  vs.  $1/[\beta\text{-CD}]$  for DPA in pH ~1 and pH ~7 solutions.



Scheme 2. The proposed structure of inclusion complex of DPA with  $\beta$ -CD for 1:1 inclusion complex.

At constant temperature

$$\Delta S = \frac{\Delta H - \Delta G}{T}$$

The thermodynamic parameters  $\Delta G$ ,  $\Delta H$  and  $\Delta S$  for the binding of the guest molecule to  $\beta$ -CD cavity are given in Table 1. As can be seen from Table 1,  $\Delta G$  is negative which suggests that the inclusion process proceeded spontaneously at 303 K.  $\Delta H$  and  $\Delta S$  are also negative in the experimental temperature range, which indicates that the inclusion process is an exergonic and enthalpy controlled process. The negative enthalpy change ( $\Delta H$ ) arose from the van der Waals interaction, while the negative entropy change ( $\Delta S$ ) is the steric barrier caused by molecular geometrical shape and the limit of  $\beta$ -CD cavity to the freedom of shift and rotation of DPA molecule. The experimental results indicated that the inclusion reaction of  $\beta$ -CD with DPA was an exothermic reaction accompanied with negative  $\Delta S$ . In this case, the actions that enthalpy and entropy change played were on the contrary. The conclusion of these thermodynamic parameters is that changes in  $\Delta H$  are largely compensated for by changes in  $\Delta S$ .

Considering the above discussions, the possible inclusion mechanism is proposed. Naturally, the inclusion complex formation between DPA and  $\beta$ -CD is possible with the imine group captured inside the  $\beta$ -CD cavity and it is shown in Scheme 2.

### 3.2. Electrochemical method

The formation of inclusion complex of DPA and  $\beta$ -CD was also confirmed by electrochemical analytical method. The electrochemical behavior of DPA has been widely researched in same observation [36]. If  $\beta$ -CD interacted with DPA, different electrochemical properties would be observed. First, some DPA was put into  $\beta$ -CD aqueous solution (pH ~1 and pH ~7) with sufficient stirring. Then the cyclic voltammograms were recorded after the solution was kept static for at least 24 h.

From Figs. 4 and 5 it is observed that the anodic peak current,  $i_{pa}$ , decreased drastically with increasing concentration of  $\beta$ -CD in both pHs (pH ~1 and pH ~7). The anodic peak potential,  $E_{pa}$ , shifted in positive direction when  $\beta$ -CD was increased in both cases. The result showed that the inclusion complex between  $\beta$ -CD and DPA was formed when  $\beta$ -CD was added into DPA aqueous solution. The diffusion coefficient of the inclusion complex from bulk layer to electrode surface was very slow than that of the DPA monomer itself, which led the current decrease. On the other hand, because DPA monomer entered into the hydrophobic cavity

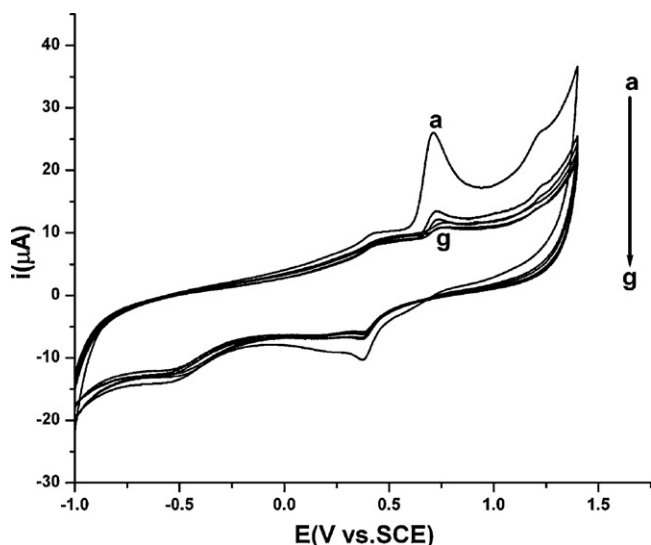


Fig. 4. CV for DPA in pH  $\sim 1$  buffer solution, scan rate  $100 \text{ mVs}^{-1}$ , DPA (Conc.  $2 \times 10^{-4} \text{ M}$ ) solution in different concentrations of  $\beta\text{-CD}$  (a) 0.0 M, (b) 0.002 M, (c) 0.004 M, (d) 0.006 M, (e) 0.008 M, (f) 0.010 M and (g) 0.012 M.

of  $\beta\text{-CD}$ , it was reasonable that the electrochemical oxidation of the inclusion complex was more difficult than that of DPA monomer itself, which would lead the anodic peak shift in positive direction, the anodic peak current,  $i_{\text{ap}}$ , decreased and also higher activation energy would be observed in both pHs.

From Tables 2 and 3 the oxidation potential of DPA is 0.710 V, 0.473 V and the reduction potential is 0.374 V, 0.159 V in pH  $\sim 1$  and pH  $\sim 7$  respectively. The difference between the oxidation and reduction potentials is 168 mV and 157 mV for pH  $\sim 1$  and pH  $\sim 7$  respectively, so this reaction in both pH media is quasi reversible. By increasing the  $\beta\text{-CD}$  concentration from  $2 \times 10^{-3} \text{ M}$  to  $12 \times 10^{-3} \text{ M}$ , the difference between the oxidation and reduction potentials is increased to 242 mV and 280 mV for pH  $\sim 1$  and pH  $\sim 7$  respectively. Because of this reaction moves towards irreversibility and because DPA monomer entered into the hydrophobic cavity of  $\beta\text{-CD}$ , it was reasonable that the electrochemical oxidation of the inclusion complex was more difficult than that of DPA itself.

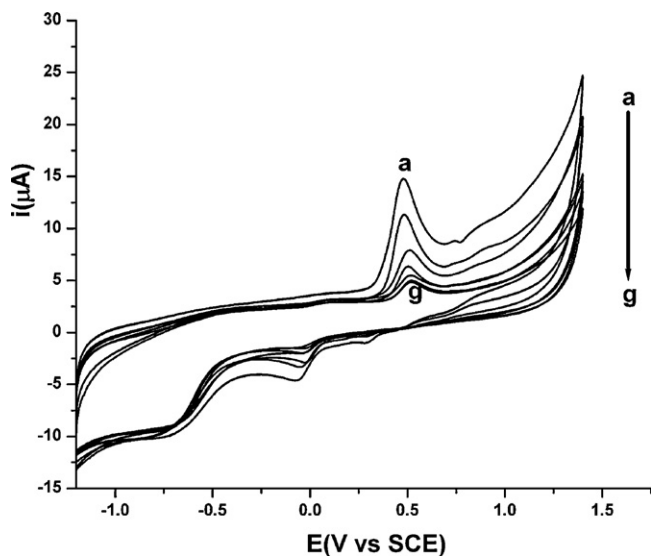


Fig. 5. CV for DPA in pH  $\sim 7$  buffer solution, scan rate  $100 \text{ mVs}^{-1}$ , DPA (Conc.  $2 \times 10^{-4} \text{ M}$ ) solution in different concentrations of  $\beta\text{-CD}$  (a) 0.0 M, (b) 0.002 M, (c) 0.004 M, (d) 0.006 M, (e) 0.008 M, (f) 0.010 M and (g) 0.012 M.

Table 2

CV for DPA- $\beta\text{-CD}$  in pH  $\sim 1$  buffer solution and scan rate  $100 \text{ mVs}^{-1}$ , DPA (Conc.  $2 \times 10^{-4} \text{ M}$ ) solution and  $0\text{--}12 \times 10^{-3} \text{ M}$   $\beta\text{-CD}$  concentrations.

$\beta\text{-CD}$ concentration (M)	$E_{\text{pa}}$ (V)	$I_{\text{pa}}$ ( $\mu\text{A}$ )	$I_{\text{pc}}$ ( $\mu\text{A}$ )	$E_{\text{pc}}$ (V)	$(E_{\text{pa}} - E_{\text{pc}})/2$ (mV)
Without $\beta\text{-CD}$	0.710	15.09	-4.28	0.374	168
0.002	0.724	4.24	-3.00	0.364	180
0.004	0.737	2.92	-3.03	0.367	185
0.006	0.754	1.65	-2.08	0.296	229
0.008	0.777	1.36	-2.93	0.375	201
0.010	0.790	0.95	-2.17	0.307	242
0.012	0.790	0.93	-2.16	0.307	243
Binding constant ( $\text{M}^{-1}$ )					964

Table 3

CV for DPA- $\beta\text{-CD}$  in pH  $\sim 7$  buffer solution and scan rate  $100 \text{ mVs}^{-1}$ , DPA (Conc.  $2 \times 10^{-4} \text{ M}$ ) solution and  $0\text{--}12 \times 10^{-3} \text{ M}$   $\beta\text{-CD}$  concentrations.

$\beta\text{-CD}$ concentration (M)	$E_{\text{pa}}$ (V)	$I_{\text{pa}}$ ( $\mu\text{A}$ )	$I_{\text{pc}}$ ( $\mu\text{A}$ )	$E_{\text{pc}}$ (V)	$(E_{\text{pa}} - E_{\text{pc}})/2$ (mV)
Without $\beta\text{-CD}$	0.473	10.690	-1.531	0.159	157
0.002	0.484	7.726	-2.162	-0.051	268
0.004	0.512	4.165	-1.709	-0.026	269
0.006	0.514	3.129	-1.136	-0.044	274
0.008	0.518	1.975	-0.922	-0.052	285
0.010	0.519	1.881	-0.901	-0.041	280
0.012	0.521	1.781	-0.789	-0.038	280
Binding constant ( $\text{M}^{-1}$ )					463

The oxidation potential of DPA in pH  $\sim 1$  is higher (0.710 V) than that in pH  $\sim 7$  (0.473 V), this is due to the formation of monocation (acidic condition) in pH  $\sim 1$ , because of this monocation oxidation observed at higher potential (0.710 V) and the peak current also increases (15.09 mV) due to loss of protonated  $\text{H}^+$ . In pH  $\sim 7$  the lone pair of electron gets oxidized at lower potential (0.473 V) and peak current also decreases (10.69 mV). In pH  $\sim 1$  system  $2e^-$  and  $1\text{H}^+$  are involved in electrochemical reaction [37] and in pH  $\sim 7$  system only  $2e^-$  is involved [37,38].

Fig. 6 shows the relationship between the anodic peak potential of DPA and the solution pH. It is found that the potentials ( $E_{\text{pa}}$ ) shifted negatively with increasing pH, indicating that protons take part in the oxidation process of DPA at the GCE surface. The anodic peak potential ( $E_{\text{pa}}$ ) is proportional to the solution pH in the range of

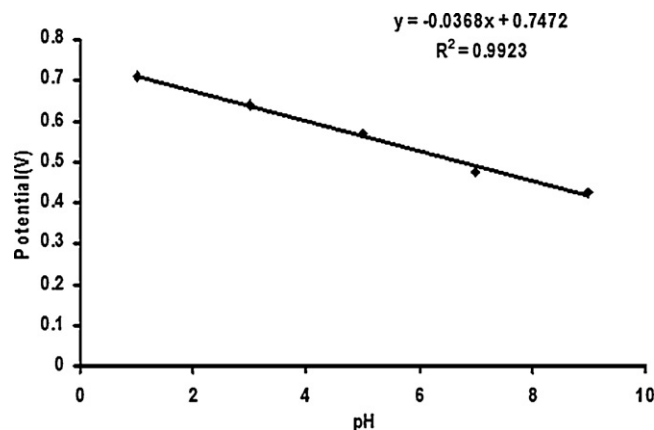
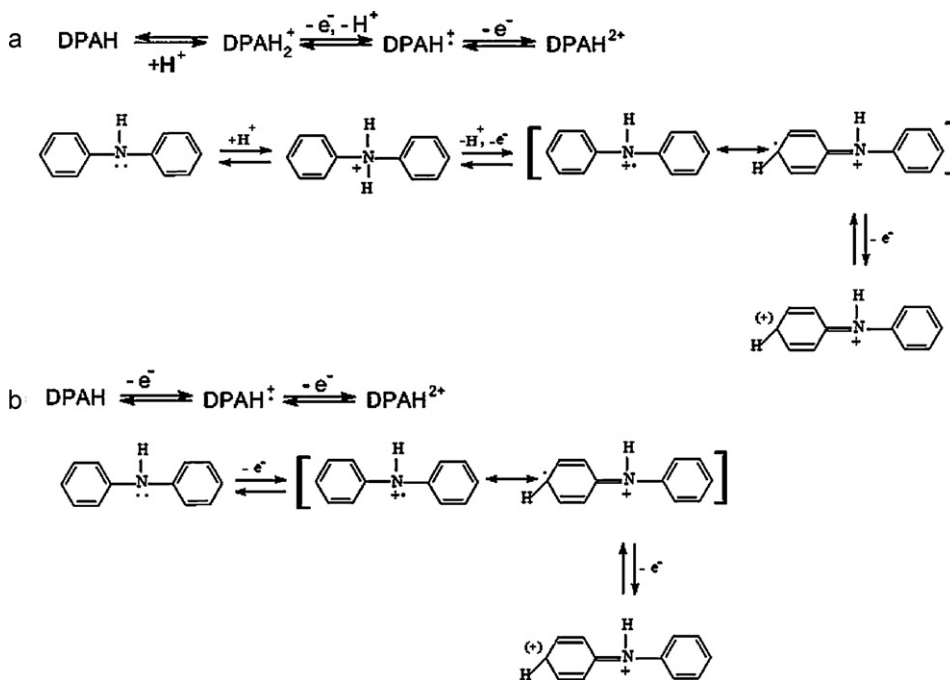


Fig. 6. The anodic peak potential ( $E_{\text{pa}}$ ) is proportional to the solution pH  $\sim 1\text{--}9$ .



Scheme 3. Electrochemical reaction mechanism of DPA, (a) pH ~1 system and (b) pH ~7 system.

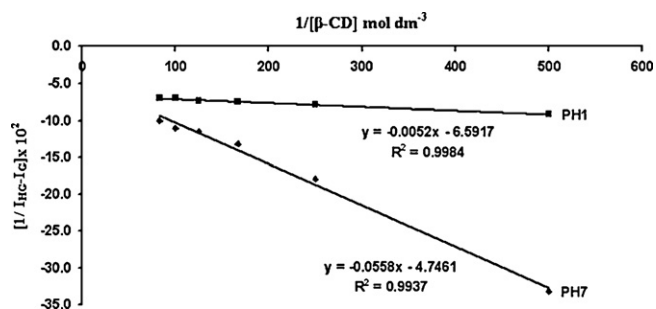


Fig. 7. Benesi-Hildebrand plot of  $1/[I_{\text{HG}} - I_{\text{G}}]$  vs.  $1/[\beta\text{-CD}]$  for DPA in pH ~1 and pH ~7.

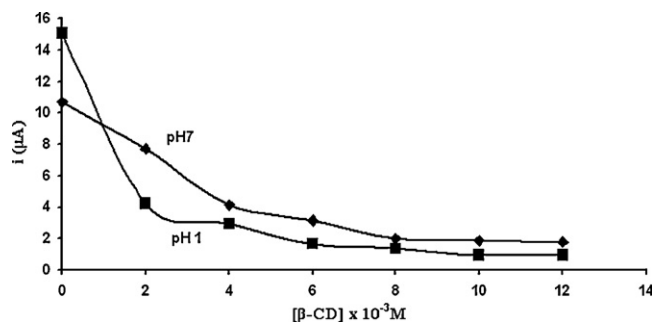


Fig. 8. The peak current of DPA changes at 0.710 V and 0.473 V with different  $\beta\text{-CD}$  concentrations in pH ~1 and pH ~7 respectively.

1–9. The linear-regression equation of DPA is described as following with a correlation coefficient of 0.9923.

$$E_{\text{pa}} (\text{V}) = 0.7472 - 0.0368\text{pH}$$

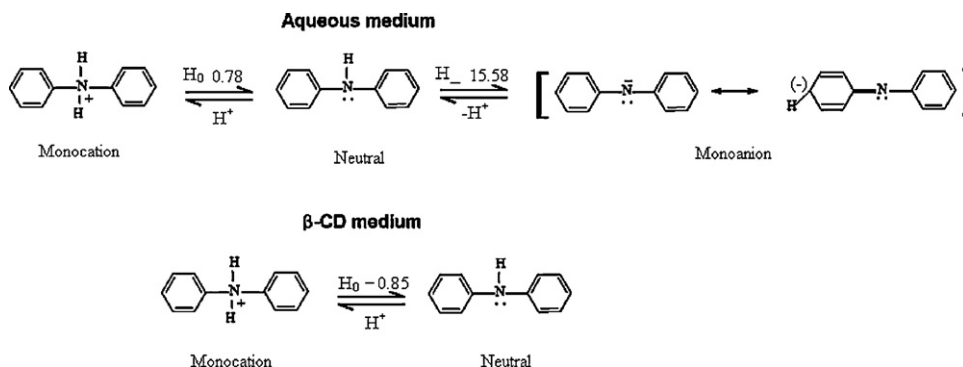
Thus the probable electrochemical reaction mechanism of DPA (denoted as DPAH) is given in Scheme 3.

The binding constant  $K$  and stoichiometric ratios of the inclusion complex of DPA can be determined according to the

Benesi-Hildebrand [35] relation assuming the formation of a 1:1 host-guest complex.

$$\frac{1}{I_{\text{HG}} - I_{\text{G}}} = \frac{1}{\Delta I} + \frac{1}{K[\text{DPA}]_0 \Delta I [\beta\text{-CD}]}$$

where  $I_{\text{G}}$  is the oxidation peak current of guest molecule of DPA, and  $I_{\text{HG}}$  is the oxidation peak current of inclusion complex of DPA- $\beta\text{-CD}$ .  $I_{\text{HG}} - I_{\text{G}}$  is the difference between the oxidation peak current



Scheme 4. Various prototropic equilibria of DPA in aqueous and  $\beta\text{-CD}$  medium.

**Table 4**  
Prototropic maxima (absorption) of DPA in with and without  $\beta$ -CD medium.

With $\beta$ -cyclodextrin			Without $\beta$ -cyclodextrin [31]	
Species	$\lambda^{\max}$ (nm)	$pK_a$	$\lambda^{\max}$ (nm)	$pK_a$
Monocation	282.0	-0.85	255.0	0.78
Neutral	283.5	2.0–15.75	279.0	2–14
Monoanion	-	-	298.4	15.58

of inclusion complex and DPA.  $\Delta I$  is the difference between the molar peak current coefficient of the inclusion complex and DPA,  $[DPA]_0$  and  $[\beta\text{-CD}]_0$  are the initial concentrations of DPA and  $\beta$ -CD, respectively.

A plot of  $[1/I_{HG} - I_G]$  vs.  $1/[\beta\text{-CD}]$  gives a straight line for both pH solutions as shown in Fig. 7. A good linear correlations were obtained, confirming the formation of a 1:1 inclusion complex for both pH solutions. From the intercept and slope values of this plot  $K$  was evaluated, the binding constant for DPA:  $\beta$ -CD is  $964\text{ M}^{-1}$  and  $463\text{ M}^{-1}$  in  $\text{pH} \sim 1$  and  $\text{pH} \sim 7$  respectively. When the  $\beta$ -CD concentrations are higher than  $8 \times 10^{-3}\text{ mol dm}^{-3}$ , the oxidation peak current remains unchanged and there is no change in the peak potential differences by further addition of  $\beta$ -CD (Fig. 8). This behavior has been attributed to the enhanced dissolution of the DPA molecule through the hydrophobic interaction between DPA and  $\beta$ -CD. These results indicate that DPA molecule is entrapped in

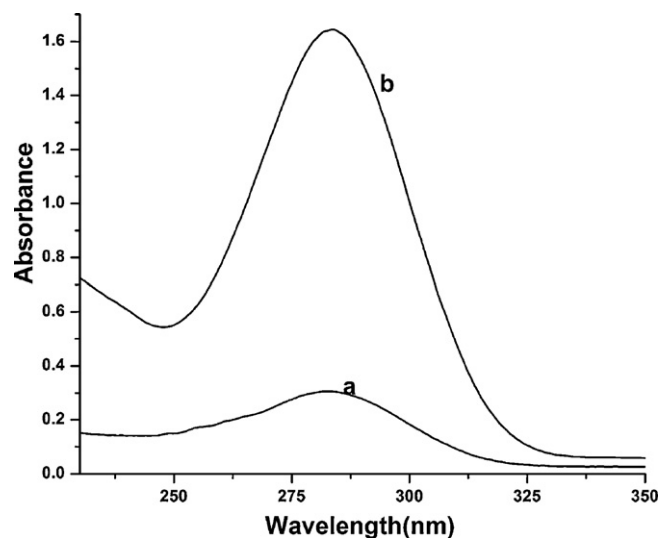


**Fig. 9.** Absorption spectra of DPA in different prototropic species at 303 K with  $\beta$ -CD (a) monocation and (b) neutral.

the  $\beta$ -CD cavity to form inclusion complex and it proved electrochemically.

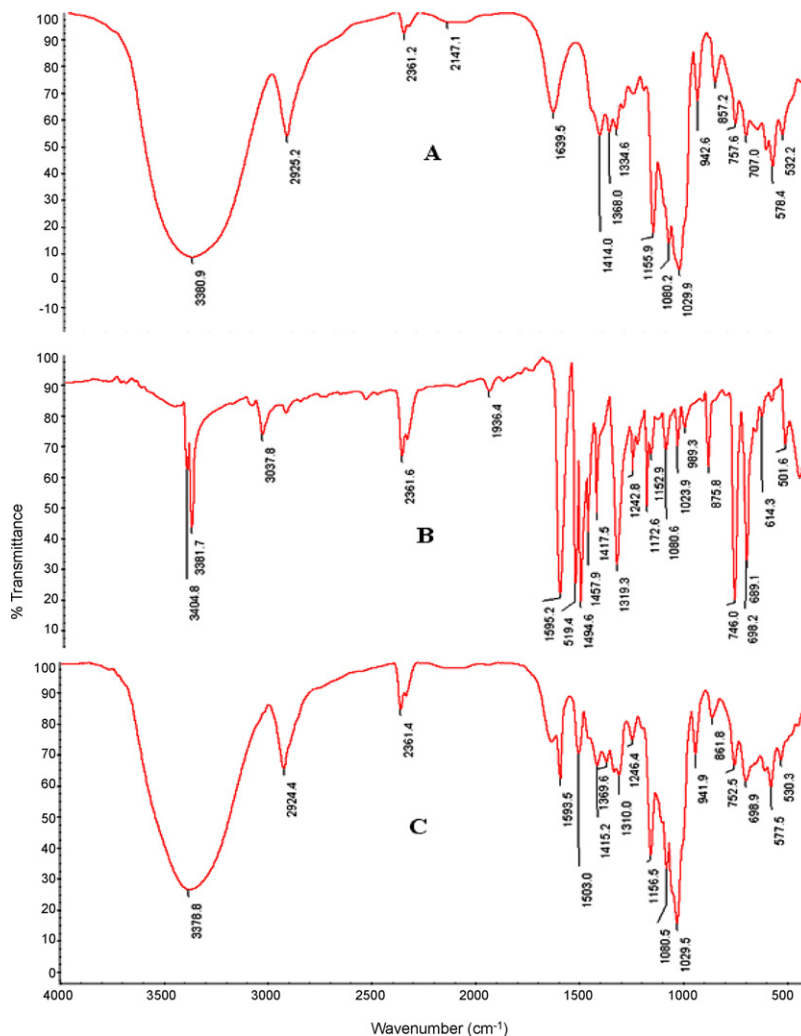
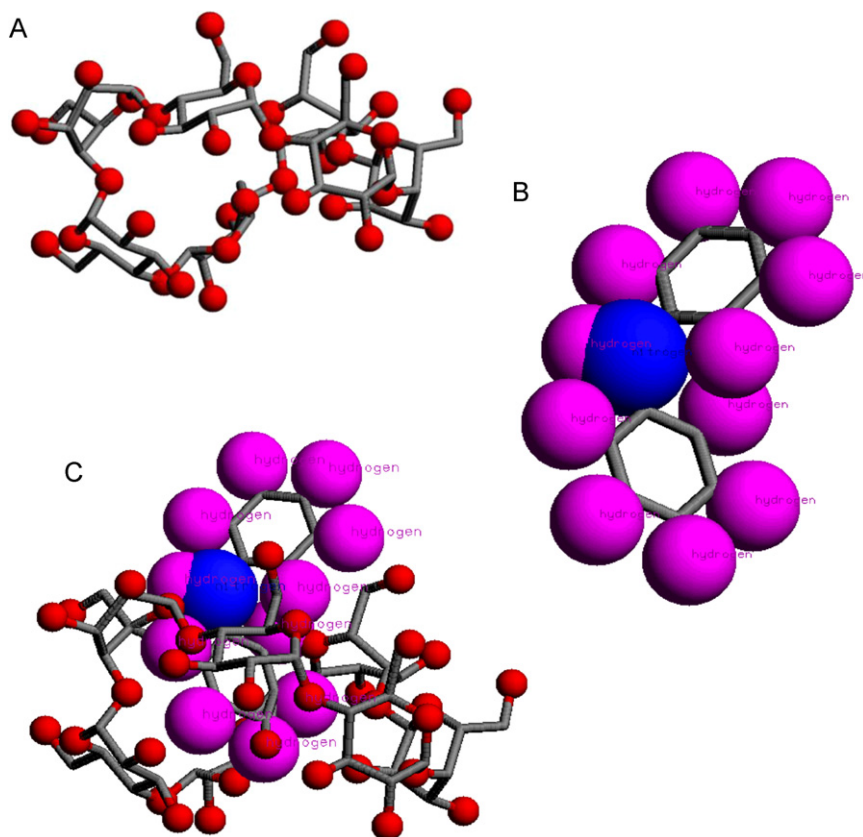


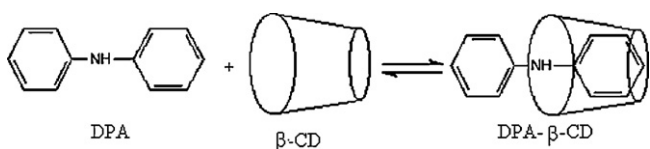
**Fig. 10.** FT-IR spectra of (A)  $\beta$ -CD, (B) DPA and (C) DPA- $\beta$ -CD solid complex in KBr.



**Scheme 5.** (A) Ball and stick representation of  $\beta$ -cyclodextrin. The oxygen atoms of  $-\text{OH}$  groups are shown as red balls, hydrogen atoms are not shown. (B) Ball and stick representation of DPA. The hydrogen atoms are shown as magenta balls and nitrogen atom as blue ball. (C) Ball and stick representation of proposed inclusion complex structure of DPA with  $\beta$ -cyclodextrin. The hydrogen atoms of DPA are shown as magenta balls and nitrogen atom as blue ball. The  $-\text{OH}$  group oxygen atoms of  $\beta$ -cyclodextrin are shown as red balls, hydrogen atoms are not shown. (For interpretation of the references to color in this figure legend, the reader is referred to the web version of the article.)

### 3.3. Effect of pH with $\beta$ -CD medium

The absorption spectra of DPA have been studied in the pH range  $H_0 - 0.84$  to  $H_- 15.75$  in  $\beta$ -CD medium. KothaiNayaki et al. [31] studied the absorption spectra of DPA in the pH range without  $\beta$ -CD,  $H_0 - 3$  to  $H_- 16$  in aqueous solution, there are three prototropic species (monocation–neutral–monoanion) present in aqueous medium. But in the case of  $\beta$ -CD medium it presents two species (Table 4 and Fig. 9) (neutral and monocation). When compared to aqueous medium there is some appreciable change in the absorption maxima of neutral to monocation (Fig. 9). The equilibrium of DPA could be due to the presence of resonating structure as shown in Scheme 4. The absorption maxima of DPA have been taken in  $12 \times 10^{-3}$  M  $\beta$ -CD aqueous solutions in the pH range ( $H_0 - 0.85$  to  $H_- 15.75$ ). Noticeable change is observed in the absorption spectral intensity, when pH was decreased below pH  $\sim 1.0$  and the absorption maximum also decreased in 2 M  $\text{H}_2\text{SO}_4$  solution. Though a new blue-shifted absorption spectrum was observed at 282 nm due to the formation of the monocation by the protonation of imino group and there is no clear isosbestic point observed for this ground state equilibrium between the cation and neutral forms.



**Scheme 6.** DPA- $\beta$ -CD 1:1 host-guest mechanism.

When pH is increased above 14 no noticeable change is observed in the absorption spectra, whereas blue shift is observed in neutral to monocation of DPA in  $\beta$ -CD when compared to aqueous (without  $\beta$ -CD) medium [31]. But the monocation is not formed above pH  $\sim 14$  in  $\beta$ -CD medium. Further the  $pK_a$  value for the monocation–neutral equilibrium of DPA in  $\beta$ -CD is higher than in aqueous medium; this finding confirms DPA molecule encapsulated in the  $\beta$ -CD cavity. Further it is confirmed by RasMol tool (Scheme 5) [27].

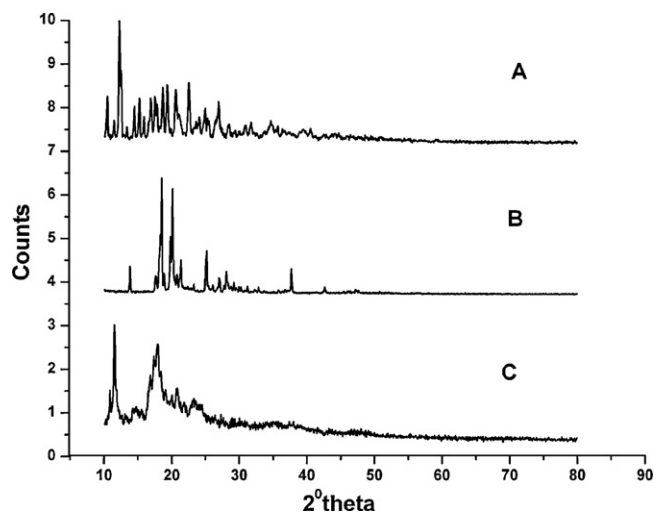


**Fig. 11.** XRD pattern of (A)  $\beta$ -CD, (B) DPA and (C) DPA- $\beta$ -CD solid complex.

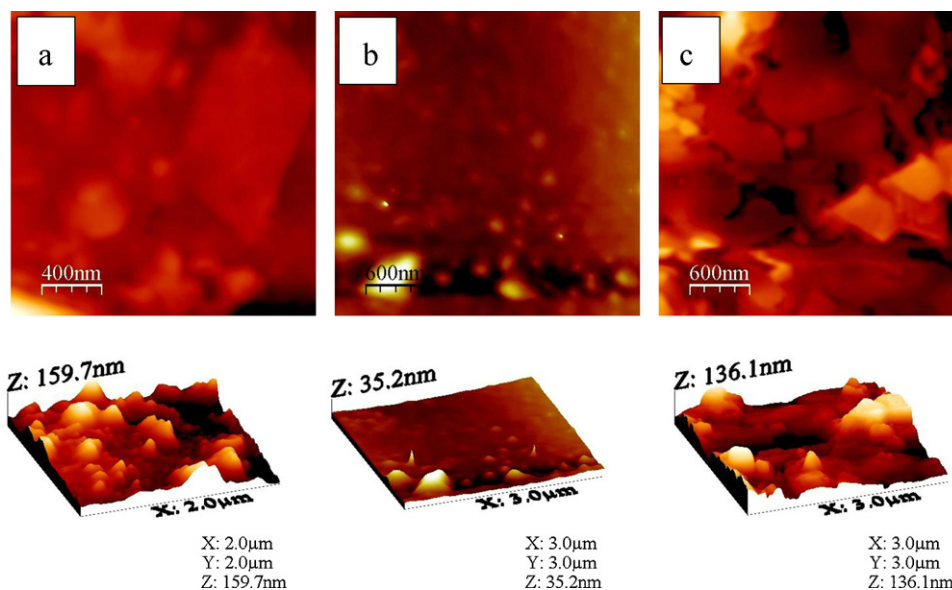


Fig. 12. Atomic force microscope photographs of (a)  $\beta$ -CD, (b) DPA and (c) DPA- $\beta$ -CD solid complex in 3D and 2D view.

### 3.4. FT-IR spectral studies

The host molecule ( $\beta$ -CD) reacts with guest molecule (DPA) to form a host-guest solid complex. The reaction sketch is as follows (Scheme 6): according to the above reaction solid complex formation may be confirmed by FT-IR spectroscopy (Fig. 10) because the bands resulting from the included part of the guest molecule are generally shifted or their intensities altered [39]. If  $\beta$ -CD and DPA form a solid inclusion complex, the non-covalent interactions between them such as hydrophobic interactions, Van der Waals interactions and hydrogen bonds lower the energy of the included part of DPA, it thus reducing the absorption intensities of the corresponding bands. We can see that there are apparent differences between the spectra of  $\beta$ -CD, DPA and solid inclusion complex. For example, the  $1595.2\text{ cm}^{-1}$  absorption peak (Fig. 10B) which could be assigned to the stretching vibration of N-H, its absorption intensity was reduced (Fig. 10C) obviously as the solid complex was formed. In addition,  $1319.3\text{ cm}^{-1}$  absorption peak which may be the C-N stretching vibration of benzene ring skeleton, its absorption intensity was reduced and shifted to  $1313.0\text{ cm}^{-1}$  (Fig. 10C) in the solid complex. Based on these facts we can conclude that hydrophobic group (>NH) of DPA is included into the  $\beta$ -CD cavity. Moreover, the absorption peak at  $746.0\text{ cm}^{-1}$  and  $698.3\text{ cm}^{-1}$  (Fig. 10B) are the characteristic peaks of monosubstituted benzene; decrease of its absorption intensity (Fig. 10C) confirms the solid complex formation. It is interested that decrease of absorption intensity N-H at  $1595.2\text{ cm}^{-1}$  proves that depth of guest molecule DPA insert into  $\beta$ -CD cavity. In the past it was thought that benzene ring was only included when the molecule containing benzene ring reacted with  $\beta$ -CD to form a supramolecular inclusion complex [40]. From the above discussions we can conclude that DPA molecule was included into  $\beta$ -CD cavity.

### 3.5. Powder X-ray diffraction spectra

The formation of the inclusion complex can be confirmed by X-ray diffractometry [41,42]. Fig. 11 shows the powder X-ray diffraction spectra of  $\beta$ -CD, DPA and solid complex. The X-ray spectrum of the inclusion complex shown in Fig. 11C was evidently different from that of  $\beta$ -CD monomer and DPA shown in Fig. 11A and B. The difference between both spectra of  $\beta$ -CD and inclusion complex is due to the interaction of  $\beta$ -CD with DPA and it formed

a new crystal structure of solid complex.

### 3.6. Atomic force microscopic morphological observations

Atomic force microscopes (AFMs) are well suited for visualizing the surface texture of the deposited films, especially when the surface feature sizes are far below three micron. The AFM analysis is ideal for quantitatively measuring the nanometric dimensional surface roughness and for visualizing the surface nano-texture of the deposited film. First we observed surface morphological structure of  $\beta$ -CD and DPA by AFM (Fig. 12a and b respectively) method, and then we also observed the surface morphological structure of solid inclusion complex (Fig. 12c). Pictures clearly elucidated the difference of each other. Modification of crystals can be assumed as a proof of the formation of a solid inclusion complex. Measuring the surface texture of  $\beta$ -CD, DPA and solid complex films with horizontal length scale of less than  $3\text{ }\mu\text{m}$  and a vertical length scale of  $159.7\text{ nm}$ ,  $35\text{ nm}$  and  $136\text{ nm}$  respectively. This solid inclusion complex formation may lead to the preparation of nanomaterials using  $\beta$ -CD.

## 4. Conclusions

The following conclusion can be arrived at from the above studies; (i) DPA forms 1:1 inclusion complex with  $\beta$ -CD (ii) prototropic reactions in  $\beta$ -CD medium indicate, NH group present in the upper rim (polar) of the  $\beta$ -CD cavity (iii) FT-IR, XRD, AFM and RasMol tool results suggest that DPA formed a solid inclusion complex with  $\beta$ -CD (iv) the above studies demonstrate that in DPA, ICT interactions play a significant role in  $\beta$ -CD aqueous/polar medium.

## References

- [1] W.S. Chung, N.J. Turro, *J. Am. Chem. Soc.* 112 (1990) 1202–1205.
- [2] W. Saenger, *Angew. Chem. Int. Ed. Engl.* 19 (1980) 344–362.
- [3] M. Chen, G. Diao, *Chemosphere* 63 (2006) 522–529.
- [4] J.M. Lehn, *Supramolecular Chemistry*, VCH, Weinheim, 1995.
- [5] D. Bonenfant, P. Niquette, R. Hausler, *Water Res.* 43 (2009) 3575–3581.
- [6] D.K. Balta, N. Arsu, *J. Photochem. Photobiol. A* 200 (2008) 377–380.
- [7] G.O. Bizzigotti, D.A. Reynolds, *Environ. Sci. Technol.* 31 (1997) 472–478.
- [8] J. Szejtli, *Cyclodextrins and Their Industrial Uses*, De Sante Edn., Paris, 1987, pp. 173–210.
- [9] Y. Gao, X. Zhao, B. Dong, S. Zhang, *J. Phys. Chem. B* 110 (2006) 8576–8581.

- [10] C. Liang, C.F. Huang, N. Mohanxy, C.J. Lu, *Ind. Eng. Chem. Res.* 46 (2007) 6466–6479.
- [11] S.O. Ko, M.A. Schlautman, E.R. Carraway, *Environ. Sci. Technol.* 34 (2000) 1535–1541.
- [12] S. Murali, S. Imajo, Y. Takahashi, *Environ. Sci. Technol.* 32 (1998) 782–787.
- [13] V. Ramamurthy, D.F. Eaton, *Acc. Chem. Res.* 21 (1988) 300–306.
- [14] M.S. Syamala, V. Ramamurthy, *Tetrahedron* 44 (1988) 7223–7233.
- [15] Z.T. Jiang, R. Li, J.C. Zhang, *J. Food Drug Anal.* 12 (2004) 183–188.
- [16] J. Garcia-Rio, R. Leis, J.C. Mejuto, *J. Phys. Chem.* 101 (1997) 7383–7389.
- [17] N.E. Polyakove, T.V. Leshina, E.O. Hand, L.D.K. Spert, *J. Photochem. Photobiol. A* 161 (2004) 261–267.
- [18] G. Astray, C.G. Barreiro, J.C. Mejuto, R.R. Otero, J.S. Gandara, *Food Hydrocolloids* 23 (2009) 1631–1640.
- [19] T. Stalin, N. Rajendiran, *Spectrochim. Acta A* 61 (2005) 3087–3096.
- [20] T. Stalin, R. Anitha Devi, N. Rajendiran, *Spectrochim. Acta A* 61 (2005) 2495–2504.
- [21] T. Stalin, N. Rajendiran, *J. Mol. Struct.* 794 (2006) 35–45.
- [22] T. Stalin, N. Rajendiran, *J. Photochem. Photobiol. A* 177 (2006) 144–155.
- [23] T. Stalin, K. Sivakumar, N. Rajendiran, *Spectrochim. Acta* 62 (2005) 991–999.
- [24] T. Stalin, N. Rajendiran, *Chem. Phys.* 322 (2006) 311–322.
- [25] (a) T. Stalin, N. Rajendiran, *J. Inclusion Phenom.* 55 (2006) 21–29;  
(b) T. Stalin, N. Rajendiran, *J. Photochem. Photobiol. A* 182 (2006) 137–150;  
(c) T. Stalin, N. Rajendiran, *Ind. J. Chem.* 45 (2006) 1113–1120.
- [26] T. Stalin, K. Srinivasan, J. Vaheethabanu, P. Manisankar, *J. Mol. Struct.* 987 (2011) 214–224.
- [27] K. Sivakumar, S. Balaji, *J. Chem. Sci.* 119 (2007) 571–579.
- [28] J. Lye, H.S. Freeman, *Colour Sci. Technol.* 2 (1999) 112–119.
- [29] Drzyzga, *Chemosphere* 53 (2003) 809–818.
- [30] N. Chattopadhyay, D. Sur, P. Purkayastha, *J. Photochem. Photobiol. A* 134 (2000) 17–21.
- [31] S. KothaiNayaki, V. Arumugam, M. Swaminathan, *Ind. J. Chem.* 30A (1991) 665–669.
- [32] M.J. Jorgenson, D.R. Hartter, *J. Am. Chem. Soc.* 85 (1963) 878–883.
- [33] G. Yagil, *J. Phys. Chem.* 71 (1967) 1034–1044.
- [34] T. Stalin, M. Shanmugam, D. Ramesh, V. Nagalakshmi, R. Kavitha, R. Rajamohan, *Spectrochim. Acta A* 71 (2008) 125–132.
- [35] H.A. Benesi, J.H. Hildebrand, *J. Am. Chem. Soc.* 71 (1949) 2703–2707.
- [36] (a) M. Chen, G. Diao, E. Zhang, *Chemosphere* 63 (2006) 522–529;  
(b) Y.B. Vassiliev, V.S. Bagotzky, O.A. Khazova, T.N. Yastrebova, T.A. Sergeeva, *Electrochim. Acta* 26 (1981) 563–577;  
(c) I. Rubinstein, *J. Electroanal. Chem.* 183 (1985) 379–386.
- [37] G. Inzelt, *J. Solid State Electrochem.* 6 (2002) 265–271.
- [38] P. Santhosh, M. Sankarasubramanian, M. Thanneermalai, A. Gopalan, T. Vasudevan, *Mater. Chem. Phys.* 85 (2004) 316–328.
- [39] L. Szenté, vol. 3, Pergamon Press, Oxford, 1996, pp. 253–278.
- [40] H.Y. Wang, J.H. Feng, Y.L. Pang, *Spectrochim. Acta A* 65 (2006) 100–105.
- [41] S. Scalia, A. Molinari, A. Casolari, A. Maldotti, *Eur. J. Pharm. Sci.* 22 (2004) 241–249.
- [42] T. Pralhad, K. Rajendrakumar, *J. Pharm. Biomed. Anal.* 34 (2004) 333–339.